RESEARCH LETTER

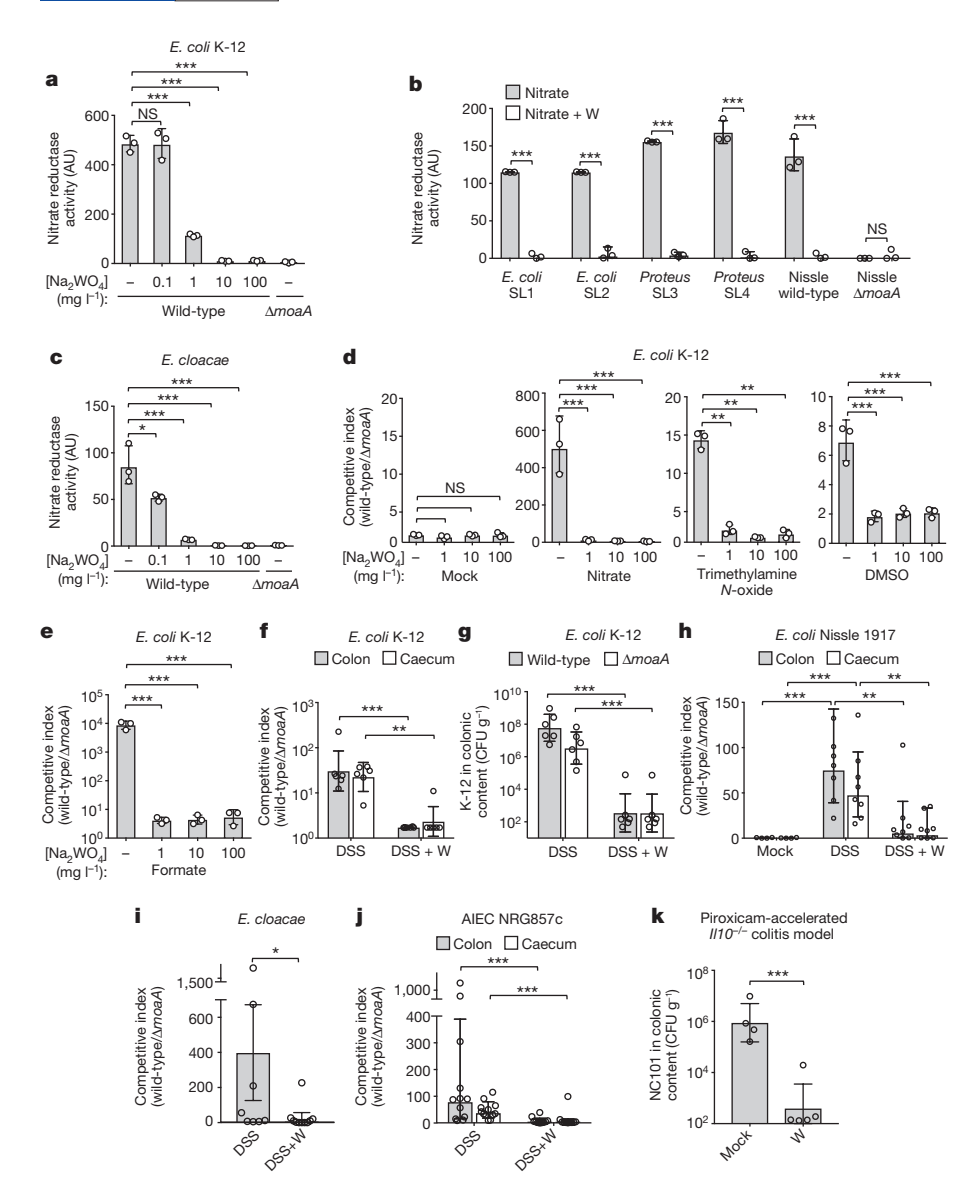


Figure 1 | Effect of tungstate on molybdenum cofactor-dependent anaerobic respiration.

a-**c** Nitrate reductase activity in E. coli K-12 (a), isolated commensal Enterobacteriaceae strains SL1-SL4 and E. coli Nissle 1917 (b; strains are described in Supplementary Table 1), and an Enterobacter cloacae strain (c). W, tungstate (Na₂WO₄); AU, arbitrary units. d, e, Competitive anaerobic growth of the E. coli K-12 wild type and a moaA mutant ($\Delta moaA$) in the presence of electron acceptors (d) or microaerobic growth with the electron donor formate (e). In \mathbf{a} - \mathbf{e} , n = 3 biological replicates for each condition. f-j, C57BL/6 mice received tungstate, DSS, or both (DSS+W) in drinking water for four days. Animals were inoculated intragastrically with an equal mixture of the indicated E. coli wild-type strains and isogenic moaA mutants. E. coli populations in the caecal and colonic content were analysed five days after inoculation: competitive index (f) and total population (g) of E. coli K-12; competitive index for Nissle 1917 (h), E. cloacae (i) and NRG857c (j). CFU, colony-forming units. In \mathbf{f} , \mathbf{g} : n = 6 per group. In \mathbf{h} : Mock, n = 4; DSS, n = 8; DSS+W, n = 8. In **i**: DSS, n = 8; DSS+W, n = 10. In **j**: DSS, n = 12; DSS+W, n = 10. k, Il10^{-/-} mice on piroxicam-fortified diet were inoculated intragastrically with the mouse strain NC101 and received tungstate in drinking water or mock treatment. The abundance of E. coli NC101 was assessed after 14 days (mock, n = 4; W, n = 5). Unless stated otherwise, n indicates the number of animals per group. Data are shown as geometric mean and geometric s.d.; *P < 0.05; **P < 0.01; ***P < 0.001; NS, not statistically significant.

the microbiota (Fig. 2a). As found in a recent metagenomic analysis of mock and DSS-treated animals¹¹, molybdenum-cofactor-dependent processes such as nitrate respiration, trimethylamine *N*-oxide respiration and formate oxidation were overrepresented¹¹ (Fig. 2b, Extended Data Fig. 5a). Tungstate administration during colitis abolished these alterations in the metagenome (Fig. 2b, Extended Data Fig. 5a). Mirroring these changes in coding capacity, tungstate treatment during DSS-induced colitis shifted the microbial community profile from a dysbiotic state towards the normal state (Fig. 2c–e, Extended Data Fig. 5b). Consistent with the idea that molybdenum-cofactor-dependent processes contribute to the inflammation-associated bloom of *E. coli* and other Enterobacteriaceae, tungstate administration selectively blunted the expansion of the Enterobacteriaceae population, whereas other major taxonomic families were only marginally affected (Fig. 2e–g, Extended Data Fig. 5c).

In the absence of inflammation, tungstate treatment did not affect the coding capacity, diversity, community structure, or population of native Enterobacteriaceae (Fig. 2c, e, f, Extended Data Figs 5b, c, 6a). Obligate anaerobic commensals such as *Bacteroides* spp. perform a rudimentary form of anaerobic respiration by reducing endogenous fumarate to succinate. The *Bacteroides* fumarate reductase is not predicted to contain a molybdenum-cofactor-binding site and tungstate treatment had no significant effect on the prevalence of predicted fumarate-reduction pathways in the microbiome (Extended Data Fig. 6b). Furthermore, *in vivo* tungstate treatment did not affect butyrate production pathways,

a major metabolic function of the microbiota (Extended Data Fig. 6c). Supplementation of growth media with tungstate did not inhibit bacterial growth or production of succinate and butyrate by *Bacteroides* and *Clostridium* strains *in vitro* (Extended Data Fig. 6d–h). We did not observe any negative effects of tungstate on the mouse host (Extended Data Fig. 7). Collectively, these experiments support the idea that tungstate inhibits the inflammation-associated changes in gut microbiota composition that are driven by molybdenum-cofactor-dependent metabolic pathways, in particular the inflammation-associated expansion of the Enterobacteriaceae population.

We then explored the consequences of tungsten-mediated microbiota editing on mucosal inflammation in the DSS-induced-colitis model. We analysed pathological changes, colon length, mRNA levels of proinflammatory markers in the caecum and proximal colon, and animal body weight in mice harbouring endogenous Enterobacteriaceae in the DSS-induced-colitis model. We also analysed mice that were experimentally colonized with *E. coli* strains K-12, Nissle 1917, AIEC NRG857c or *E. cloacae*. Administration of tungstate significantly reduced inflammatory markers and pathological changes in the large intestinal mucosa, rescued the inflammation-associated reduction of colon length and ameliorated body weight loss (Fig. 3a–c, Extended Data Figs 2c–l, 3c–h, 4d–h). This was not due to reduced DSS intake during treatment (Extended Data Fig. 8a). Similarly, tungstate administration in a piroxicam-accelerated *Il10*^{-/-} colitis model reduced intestinal inflammation (Fig. 3d–g). These findings raised the possibility that